Convective Magnetic Flux Emergence Simulations from the Deep Solar Interior to the Photosphere: Comprehensive Study of Flux Tube Twist

Shin Toriumi et al., ApJ (2024)

Donghui Son

Kyung Hee University

April 4, 2025

Solar Physics Journal Club @ KHU

KYUNG HEE
UNIVERSITY

Purpose of this study

Investigate how varying initial twist in deeply rooted magnetic flux tubes influences their emergence, helicity injection, and sunspot formation.

KYUNG HEE UNIVERSITY

Background

- Sunspots and Active Regions (ARs) arise when toroidal magnetic flux tubes formed in the convection zone rise to the photosphere.
- As a magnetic flux emerges, it supplies **magnetic helicity** to the corona, thereby accumulating free magnetic energy and ultimately triggering explosive events such as **flares**.
- The **twist** of emerging magnetic flux is highlighted as a key factor governing generation, transport, and release of a magnetic field.

This study focuses on the role of magnetic twist in the process.

KYUNG HEE UNIVERSITY

Importance of magnetic twist in emerging flux

Without sufficient twist, a flux tube can be shredded by surrounding convective flows and fail to reach the photosphere.

A certain level of twist has been considered essential for **magnetic integrity**.

Key findings from previous MHD simulations

- Twisted flux tubes emerge with distinct positive/negative polarity pattern (i.e., yin-yang pattern called “magnetic tongues”)
  - → tilt angle of the two spots
  - → sunspot rotation
  - → injecting free energy and magnetic helicity into the corona
- Higher initial twist:
  - → faster rise through the CZ
  - → more pronounced sunspot rotation
  - → stronger free energy injection

KYUNG HEE UNIVERSITY

Examples of yin-yang pattern

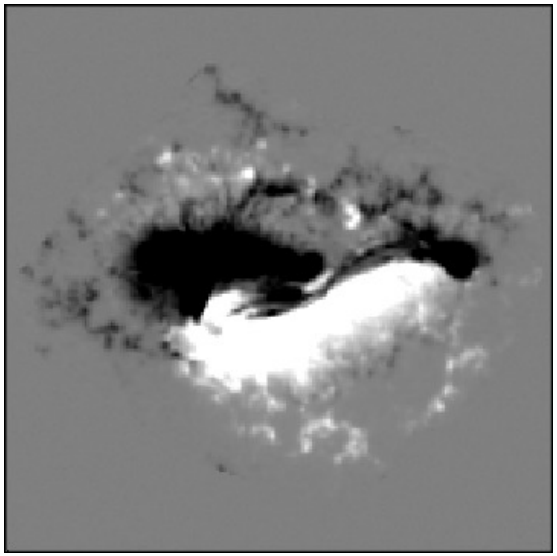

(a)

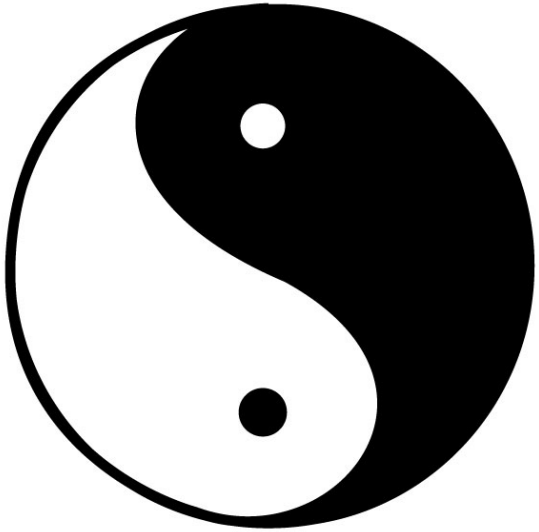

(b)

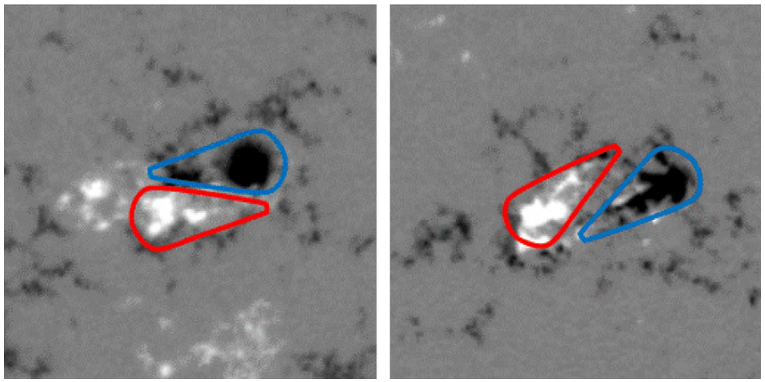

(c)

KYUNG HEE UNIVERSITY

Flare-active ARs and complex magnetic fields

- Observations show highly flare-productive ARs often have:
  - → Complex magnetic configurations
  - → δ-type sunspots (opposite polarities in one penumbra)

- Kink Instability Hypothesis:
  - → Occurs when twist exceeds critical threshold
  - → Causes flux tube to writhe and deform
  - → Can produce complex δ-spot structures

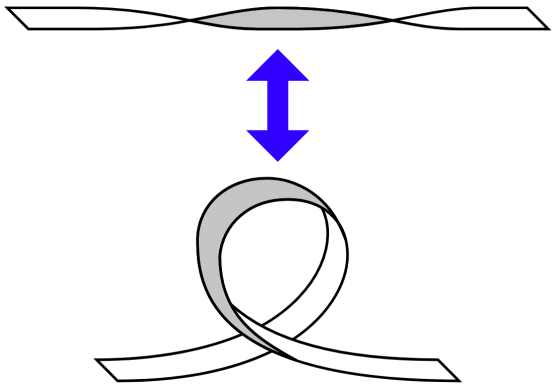

Figure 2: Helical kink instability. Conversion of twist and writhe.

KYUNG HEE UNIVERSITY

Previous studies

Key previous findings

- Tanaka (1991): δ-spots from twisted ropes
- Linton et al. (1996, 1999): Theoretical kink criterion
- Fan (1998, 1999): Kink produces writhing tubes
- Takasao et al. (2015): Kink drives polarities rotation
- Toriumi & Takasao (2018): Kink supplies the greatest free energy.
- Knizhnik et al. (2018): Tested extreme twist values (up to $4q_{cr}$)

Limitation in previous studies

Most prior models did not account for realistic convective turbulence

KYUNG HEE UNIVERSITY

Is kink instability genuinely feasible under realistic solar conditions?

What sets this study apart

- Incorporates realistic solar **thermal convection**
- Tests twist values from zero to twice kink threshold

KYUNG HEE UNIVERSITY

Radiation and Reduced Speed of Sound Technique for Deep Dynamics

$$\frac{\partial \rho_1}{\partial t} = -\frac{1}{\xi^2}\,\nabla\cdot(\rho\,\mathbf{V}),$$

$$\frac{\partial \rho_1}{\partial t} = -\,\nabla\cdot(\rho\,\mathbf{V}\,\mathbf{V}) \;-\; \nabla p_1 \;+\; \rho_1\,\mathbf{g} \;+\; \frac{1}{4\pi}\Big((\nabla\times\mathbf{B})\times\mathbf{B}\Big),$$

$$\frac{\partial \mathbf{B}}{\partial t} = \nabla\times(\mathbf{V}\times\mathbf{B}),$$

$$\rho\,T\,\frac{\partial s_1}{\partial t} = \rho\,T(\mathbf{V}\cdot\nabla)s \;+\; Q,$$

$$p_1 = p_1(\rho, s).$$

$$\rho = \rho_0 + \rho_1,$$

$$p = p_0 + p_1,$$

$$s = s_0 + s_1.$$

KYUNG HEE UNIVERSITY

Numerical model: R2D2

- Self-consistently simulates **convective motions** and **radiative transfer** throughout the solar convection zone.
- Adopts the **Model S** solar structure (for density, pressure, temperature stratification) as an initial static background, along with a realistic equation of state including **partial ionization**.
- **Radiative transfer** is solved using a gray approximation and Rosseland mean opacity in both upward and downward directions, enabling accurate modeling of **photospheric cooling** and **internal heating**, thus driving convection.

KYUNG HEE UNIVERSITY

Numerical model: R2D2

Domain specifications

- 3D Cartesian grid:
  - → $(L_x, L_y, L_z) = (98.3\ \text{Mm}, 98.3\ \text{Mm}, 201.7\ \text{Mm})$
  - → $(N_x, N_y, N_z) = (1024, 1024, 384)$: non-uniform grids for Δz
- Boundary conditions:
  - → Periodic boundaries horizontally
  - → Potential field (open) boundary at top ($z = 700$ km above the $\tau = 1$ surface)
  - → Stress-free at bottom boundary ($z = 201$ Mm below the $\tau = 1$ surface):
    - ◇ Upward convective (thermal) flux is supplied, mimicking the Sun's radiative energy input from below.
    - ◇ Open for downward flow

KYUNG HEE UNIVERSITY

Reduced speed-of-sound technique

- In the CZ, sound speed (c_s) is extremely high, making a direct simulation with full compressibility prohibitively time-consuming.
- Artificially reduces $c_s \rightarrow$ Relaxes the CFL condition $\rightarrow$ Reduces Δt constraint

The RSST factor ξ

$$\xi(z) = \max\left(1, \xi_0 \left[\frac{\rho_0(z)}{\rho_\mathrm{b}}\right]^{1/3}, \frac{c_\mathrm{s}(z)}{c_\mathrm{b}}\right), \quad c_\mathrm{s}(z) = \sqrt{(\partial p/\partial \rho)_\mathrm{s}}$$

- $\xi_0 = 160$ is a constant factor
- $\rho_b = 0.2$ g cm^{-3} is the density around the bottom of the CZ
- $c_b = 2.2 \times 10^7$ cm s^{-1} is the sound speed around the bottom of the CZ
- $c_s(z)$ is the local adiabatic sound speed.

KYUNG HEE UNIVERSITY

Simulation methodology

1. **Initial hydrodynamic phase:**
   - → Starts with magnetically free convection simulation
   - → Imposes heat flux at lower boundary
   - → Top boundary radiates energy away
2. **Development of natural convection:**
   - → System evolves to statistically steady state
   - → Forms large-scale downflow plumes and upflow cells
   - → Creates realistic solar convective environment
3. **Magnetic flux introduction:**
   - → Horizontal flux tube inserted into established convective flow
   - → Various twist parameters tested (from zero to twice kink threshold)

KYUNG HEE UNIVERSITY

Initial magnetic flux tube

Horizontal magnetic flux tube into the domain at about 20-30 Mm below the surface

$$B_x(r) = B_{\rm tb} \exp\left(-\frac{r^2}{R_{\rm tb}^2}\right), \quad B_\phi(r) = qrB_{\rm tb}(r)$$

- $B_{\rm tb}$: axial field strength
- r: radial distance from the center of the tube
- ϕ: azimuthal angle
- $R_{\rm tb}$: tube radius
- q: twist strength

$\rightarrow$ **Gaussian flux tube**

KYUNG HEE UNIVERSITY

Initial magnetic flux tube

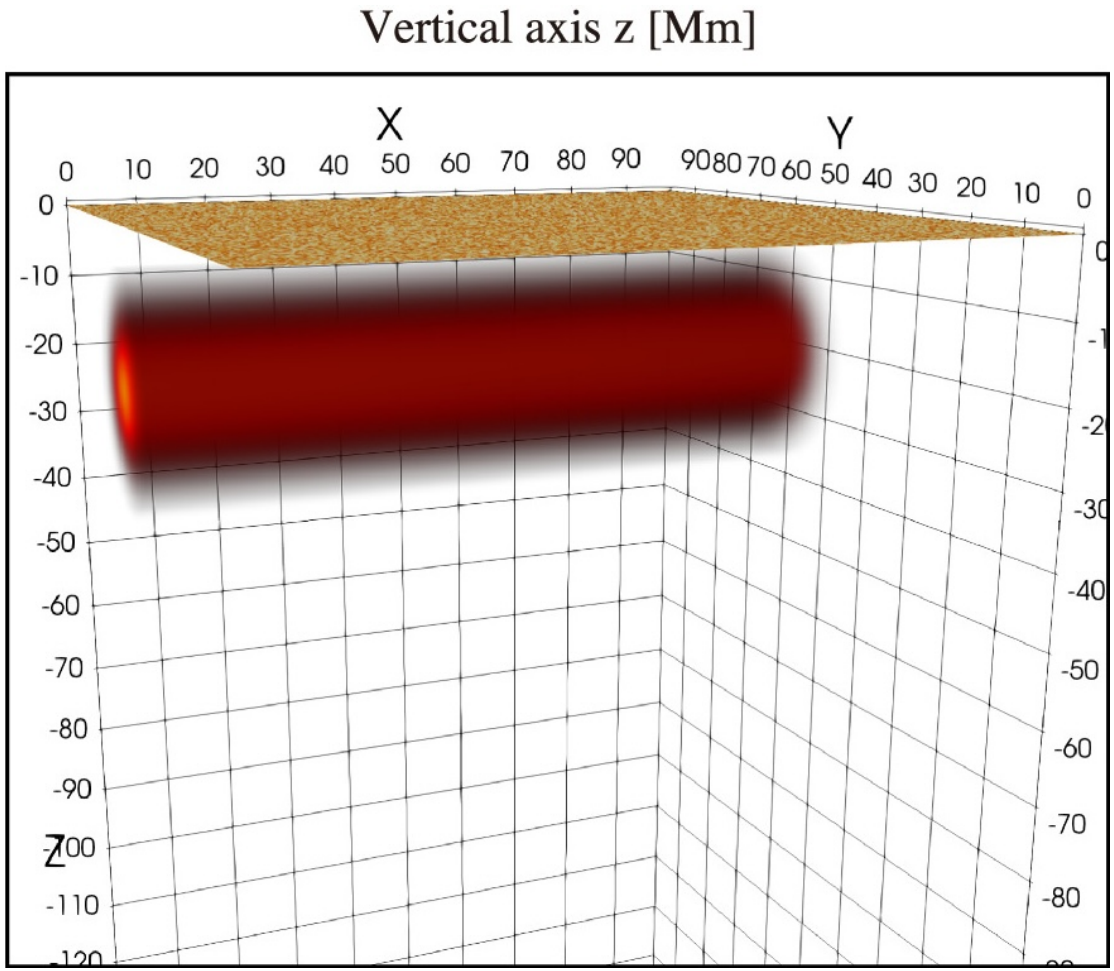

Figure 3: The total magnetic field strength for the $q/q_{cr} = 0$ case at $t = 0$ hr.

KYUNG HEE UNIVERSITY

No initial buoyancy

$$\delta p_{\rm exc} = \frac{B_x^2(r)}{8\pi}\left[q^2\left(\frac{R_{\rm tb}^2}{2}\right) - 1\right] (< 0)$$

The tube is placed in pressure balance with its surroundings, adjusting entropy so that the tube is neither more nor less dense than exterior fluid.

$\rightarrow$ **Advected by external flows**

KYUNG HEE UNIVERSITY

Simulation cases

- Nine total simulation cases
  - → $q/q_{cr} = [-2, -1, -1/2, -1/4, 0, +1/4, +1/2, +1, +2]$ with $q_{cr} = 1/R_{tb}$
  - → Positive/negative values represent right-/left-handed twists.
  - → $|q/q_{cr}| \geq 1$ indicates kink-unstable.
- Adjust the axial field strength ($B_{\rm tb}$) to maintain the same total E_{mag}
- All cases have the same initial $E_{mag} = 5.85 \times 10^{34}$ erg

Case	$B_{\rm tb}$ (kG)	$R_{\rm tb}$ (Mm)	$q/q_{\rm cr}$	q (Mm^{-1})	Φ_x (Mx)
1	7.1	8.0	-2	-0.25	1.40×10^{22}
2	10.0	8.0	-1	-0.125	1.97×10^{22}
3	11.5	8.0	$-1/2$	-0.0625	2.28×10^{22}
4	12.1	8.0	$-1/4$	-0.03125	2.38×10^{22}
5	12.2	8.0	0	0	2.42×10^{22}
6	12.1	8.0	1/4	0.03125	2.38×10^{22}
7	11.5	8.0	1/2	0.0625	2.28×10^{22}
8	10.0	8.0	1	0.125	1.97×10^{22}
9	7.1	8.0	2	0.25	1.40×10^{22}

KYUNG HEE UNIVERSITY

Analysis methodology

- **Measurement height**: $z = 200$ km (due to strong downflow at $\tau = 1$)
- **Temporal averaging**: 6-hr moving average applied to all time series data
  - → Filters out short-term convective fluctuations (10 min to few hrs)
  - → Preserves emergence dynamics (typical duration: 30-40 hr)
- **Total unsigned magnetic flux** $\Phi = \int_S |B_z| \, dS$
- **Sunspot area** A_{spot}:
  - → Regions whose emergent intensity is less than 90% of the quiet-Sun average
- **Twist parameters** (used only for $|B_z| \geq 100$ G):
  - → $\alpha_{av}^0 = \langle J_z / B_z \rangle$
  - → $\alpha_{av}^1 = \langle J_z sgn(B_z) \rangle \, / \, \langle |B_z| \rangle$
  - → $\alpha_{av}^2 = \langle B_z J_z \rangle \, / \, \langle B_z^2 \rangle$

KYUNG HEE UNIVERSITY

Analysis methodology

- **Magnetic helicity flux**: $F_z = 2\int_S \left[(\boldsymbol{A}_\mathrm{p} \cdot \boldsymbol{B}_\mathrm{h})\, V_z - (\boldsymbol{A}_\mathrm{p} \cdot \boldsymbol{V}_\mathrm{h})\, B_z\right] dS$
- **Total injected helicity**: $H_\mathrm{R} = \int_0^t F_z\, dt'$
  $\rightarrow$ a close relation with the occurrence of flares
- **Poynting flux**: $S_z = \dfrac{1}{4\pi}\displaystyle\int_S \left[B_\mathrm{h}^2\, V_z - (\boldsymbol{B}_\mathrm{h} \cdot \boldsymbol{V}_\mathrm{h}) B_z\right] dS$
- **Total injectied magnetic energy**: $E_\mathrm{mag} = \int_0^t S_z\, dt'$
  $\rightarrow$ injection of magnetic energy into the atmosphere

KYUNG HEE UNIVERSITY

Results: Overall evolution

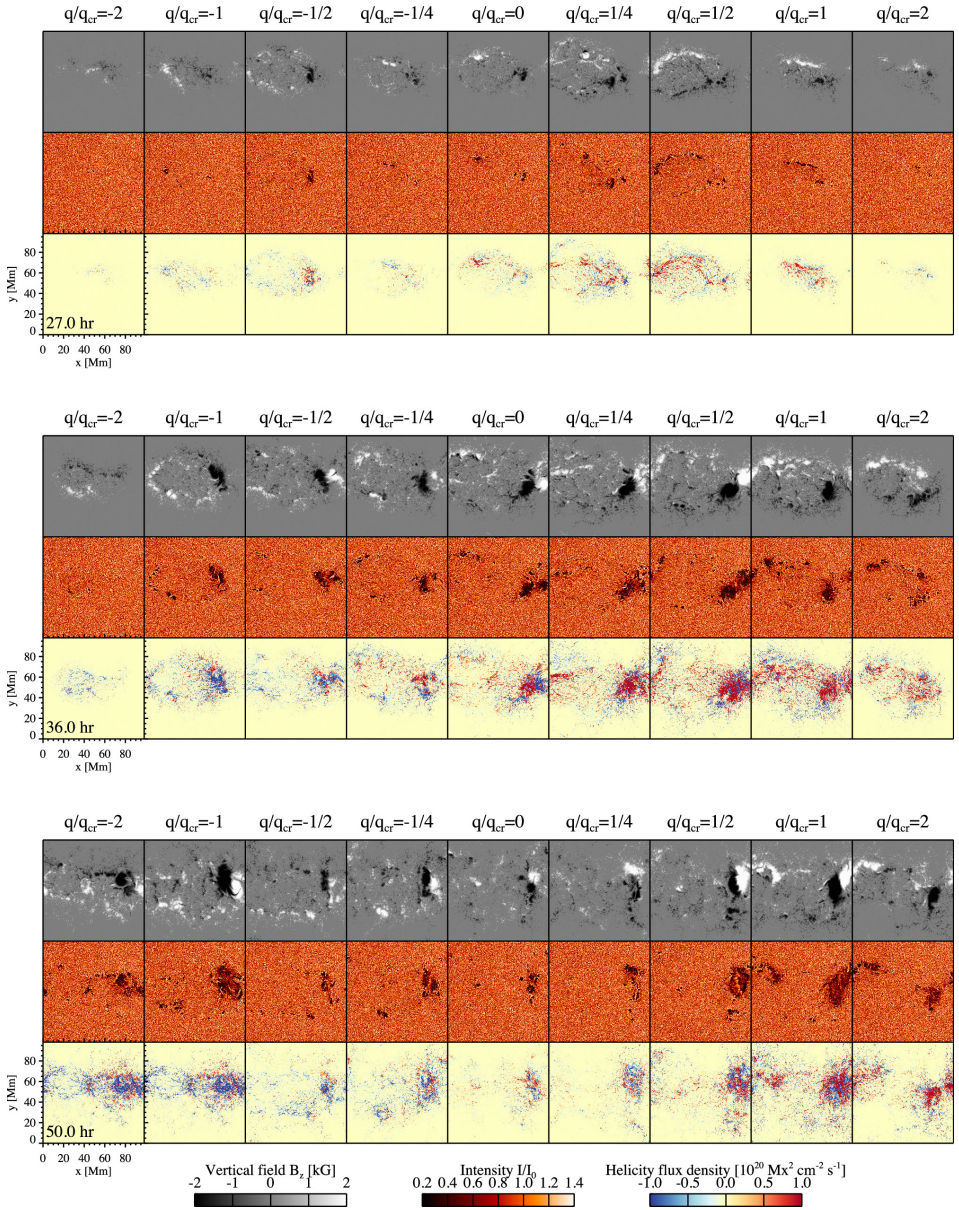

KYUNG HEE UNIVERSITY

Temporal overview

- Early stage: small fragments of the rising flux tube appear at the surface.
- $t \sim 20$ hr: the main portion emerges via large upflows.
- Emergence forms a yin-yang pattern of postive/negative polarities.
- With periodic boundaries, opposite polarities eventually collide ($t \sim 30$ hr), forming δ-spots ($t \sim 50$ hr).

Key features: an initial tilt of the untwisted case

a yin-yang pattern alone does not prove the tube was twisted
$\rightarrow$ strong turbulence can yield similar appearances even if $q = 0$.

KYUNG HEE UNIVERSITY

Effect of twist strength q/q_{cr}

- Even an untwisted tube can rise via convection.
- Weakly twisted fields diffuse quickly in the surface.
  - $\rightarrow$ the twist binds magnetic flux against turbulent shredding.
- Extremely large twist ($q/q_{cr} = \pm 2$) also shows a diffuse distribution.
  - $\rightarrow$ Initially B_{tb} is weaker.
  - $\rightarrow$ Total Φ_x is smaller.
  - $\rightarrow$ Relatively easily influenced by the surrounding turbulence.
- The sign of helicity injection depends on the twist direction.

KYUNG HEE UNIVERSITY

Results

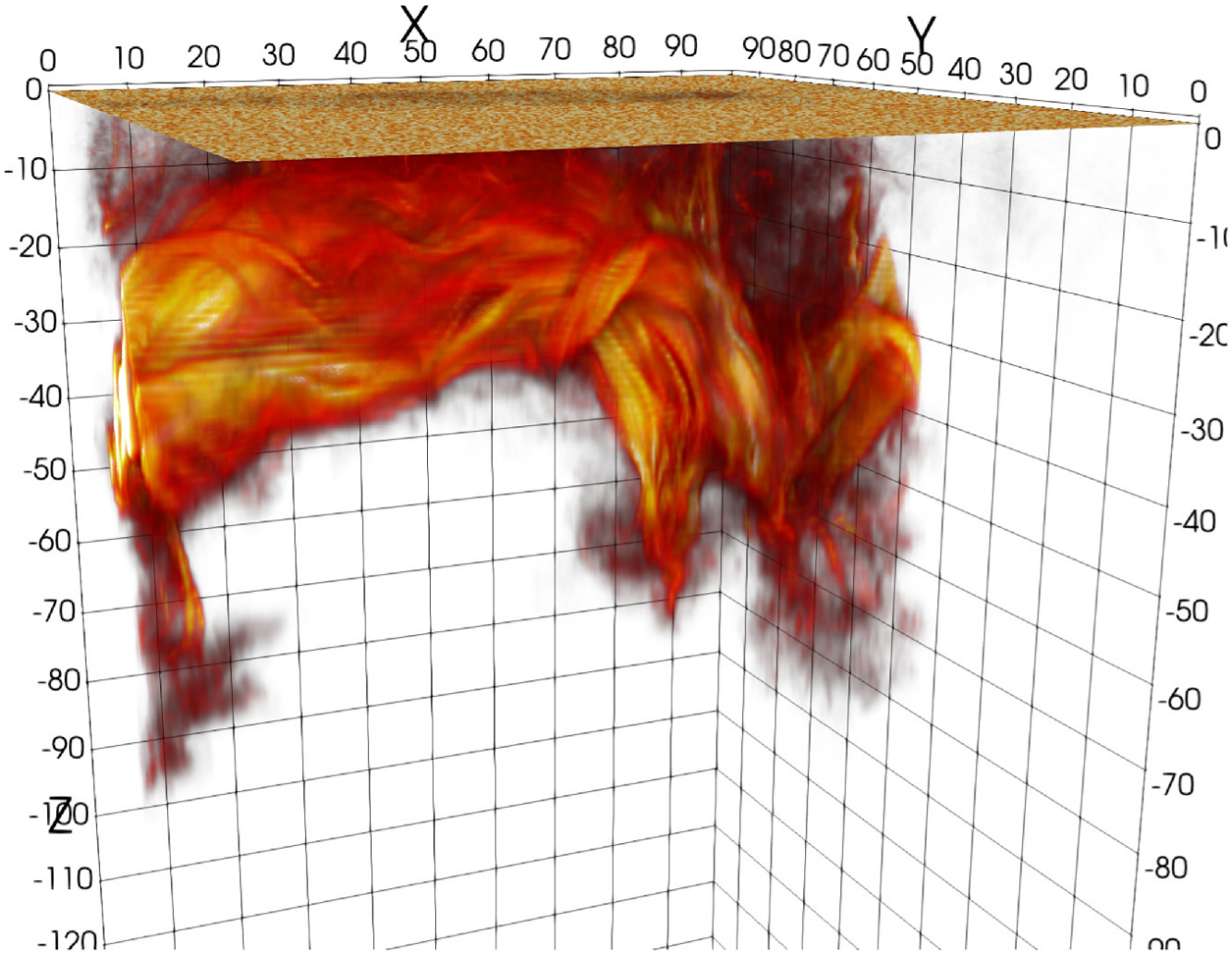

Figure 4: $|\mathbf{B}|$ at $t = 24$ hr for the $q/q_{cr} = 0$ case.

KYUNG HEE UNIVERSITY

Results: (unsigned) Magnetic flux and sunspot area

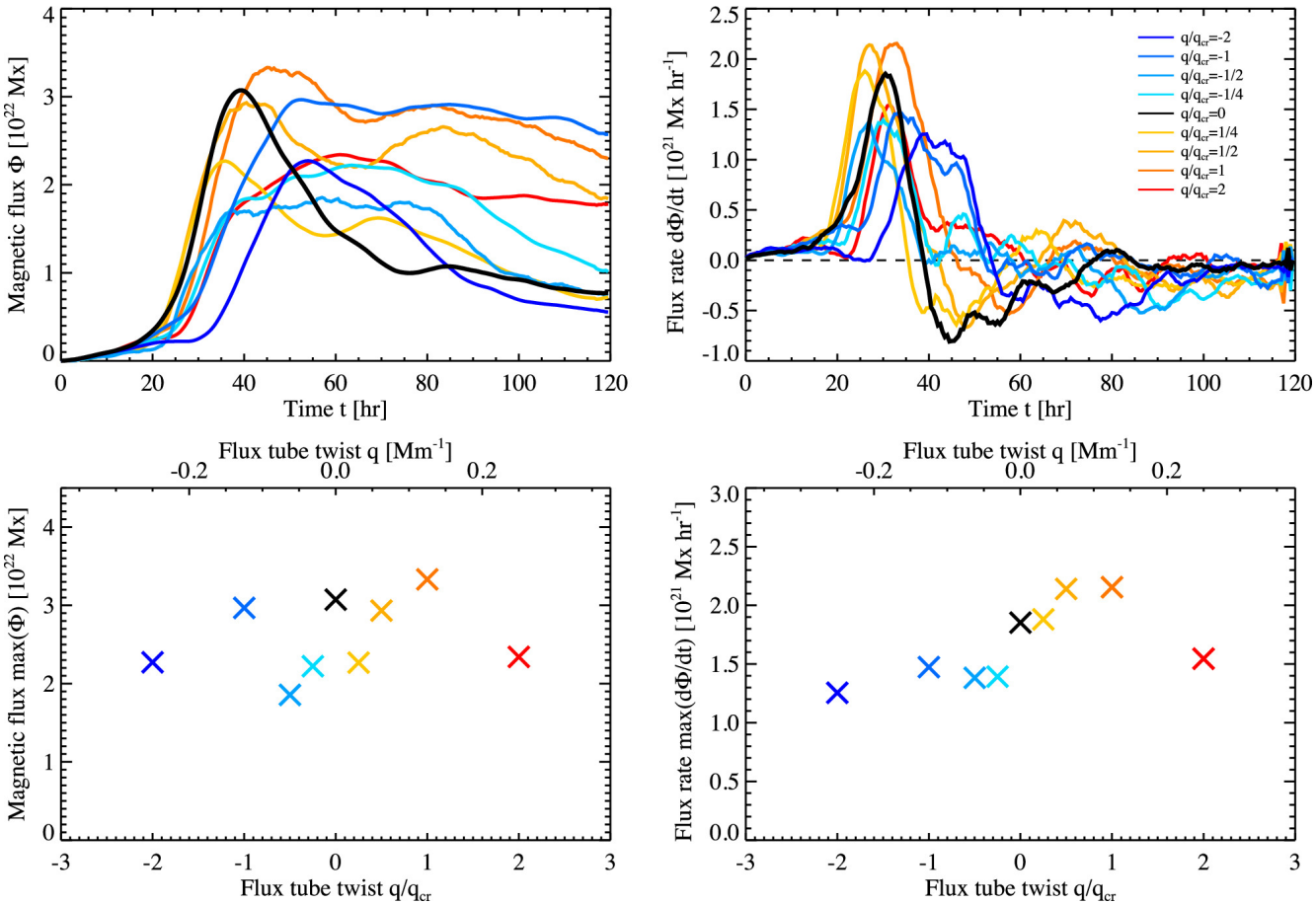

Figure 5: Temporal evolutions of the total magnetic flux, Φ, and the flux growth rate, $d\Phi/dt$, in the PH.

Effect of twist strength q/q_{cr}

- Extremely high twist ($q/q_{cr} = \pm 2$) yields a lower flux peak.
  - $\rightarrow$ $B_{eq} = 6.5$ kG at $z_{tb} = -22$ Mm
  - $\rightarrow$ $B_{tb} = 7.1$ kG, comparable to B_{eq}
  - $\rightarrow$ Easily collapsed by the external turbulent flows.

KYUNG HEE UNIVERSITY

Results: (unsigned) Magnetic flux and sunspot area

The tendency that an emerging AR with a weaker twist is more scattered, and thus has a smaller amount of magnetic flux within the spots.

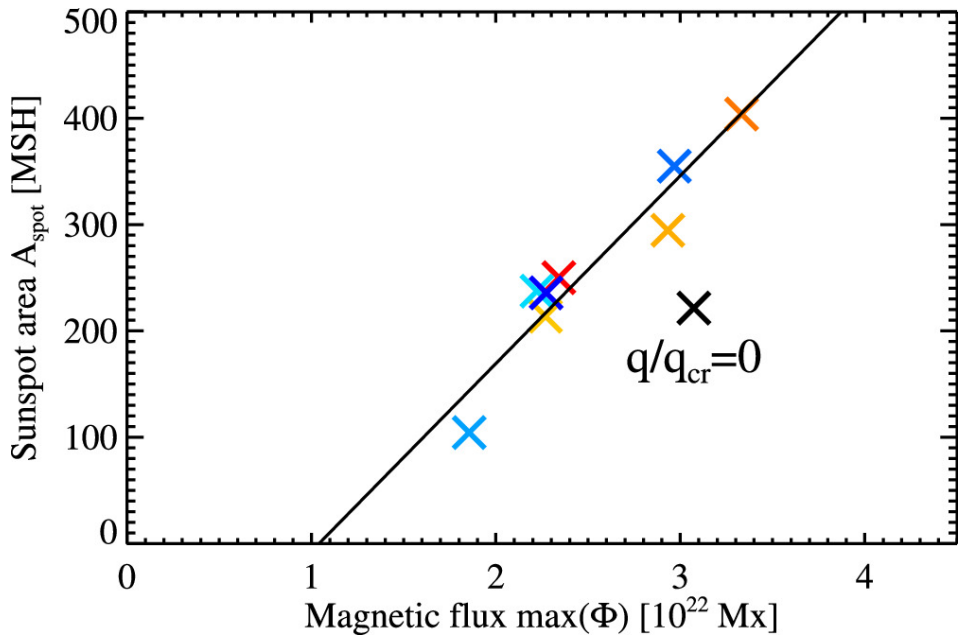

Figure 6: Maximum photospheric magnetic flux and the corresponding sunspot area. The straight line is the linear fit to the eight data points except for the untwisted flux tube.

KYUNG HEE UNIVERSITY

Results: (unsigned) Magnetic flux and sunspot area

- Numerical models tend to exhibit higher flux growth rates than observed values.
- X. Sun & A. A. Norton (2017) reported $d\Phi/dt = 4.93 \times 10^{20} \sim 10^{21}$ Mx hr^{-1} for $\Phi = 6.08 \times 10^{22}$ Mx in NOAA AR 12673.

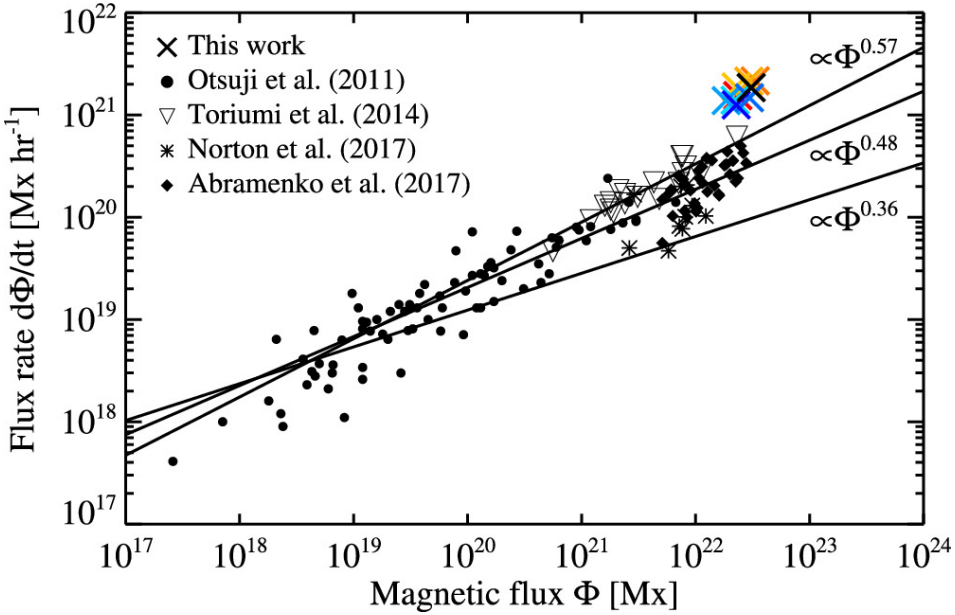

Figure 7: Flux growth rate, $d\Phi/dt$, vs. total magnetic flux, Φ, for various observations and the present nine simulation cases.

KYUNG HEE UNIVERSITY

Results: magnetic twist α_{av}

Examine how much of the twist in the initial flux tube is successfully transported to the photosphere by flux emergence

$$\alpha_{av}^{0} = \langle J_z / B_z \rangle \,,$$
$$\alpha_{av}^{1} = \langle J_z sgn(B_z) \rangle \,/\, \langle |B_z| \rangle \,,$$
$$\alpha_{av}^{2} = \langle B_z J_z \rangle \,/\, \langle B_z^2 \rangle$$

KYUNG HEE UNIVERSITY

Results: magnetic twist α_{av}

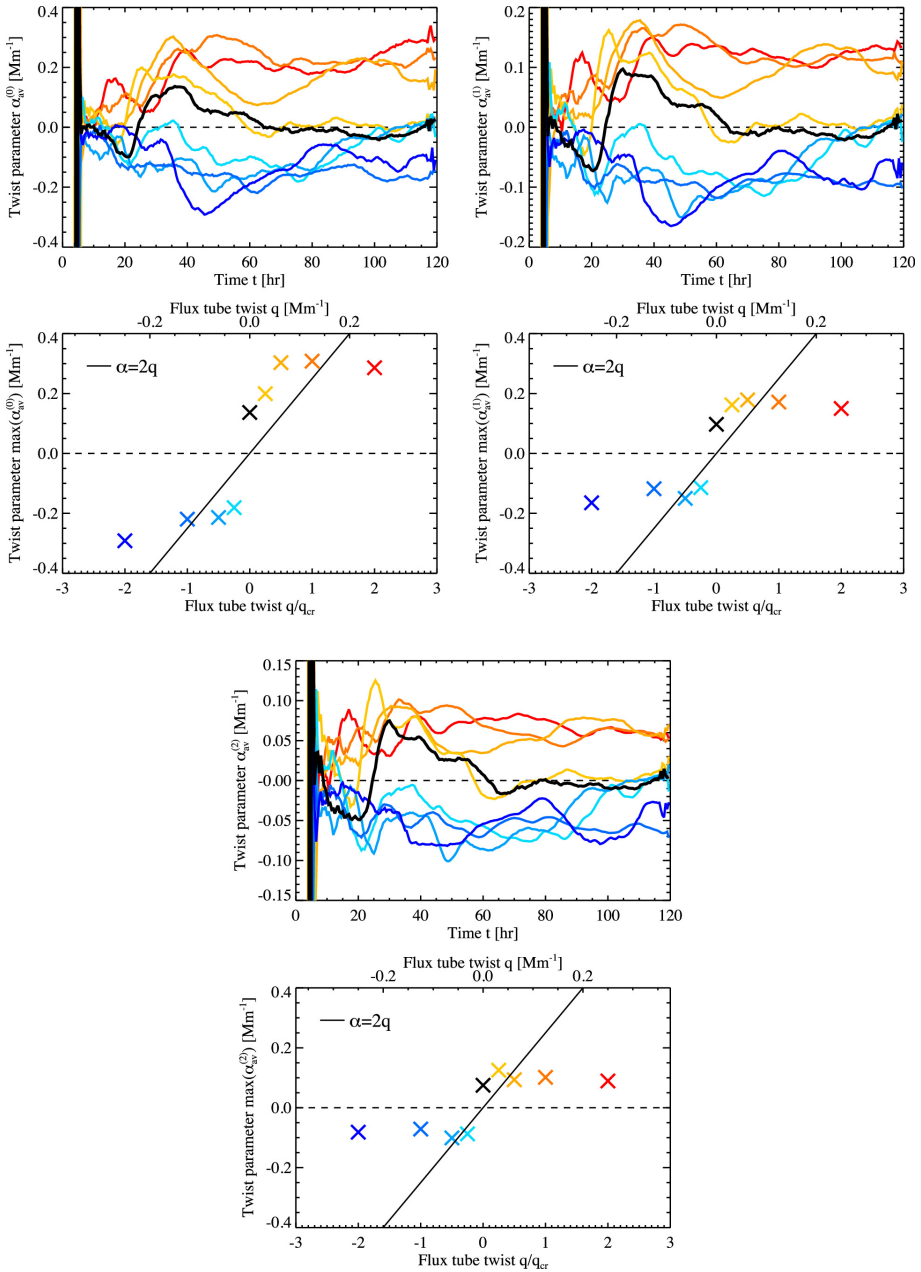

KYUNG HEE UNIVERSITY

Results: magnetic twist α_{av}

- $max(\alpha_{av})$ tends to decrease from α^0_{av} to α^2_{av}
- Considering that α^2_{av} puts the largest weight to the strong-field regions, this tendency may indicate that the weak field regions have a relatively large amount of magnetic twist.
- Smaller $|q| \rightarrow$ conserves the original twist better
- Higher $|q| \rightarrow \alpha_{av}$ becomes saturated
  - $\rightarrow$ less successful emergence of strong-twist cases
  - $\rightarrow$ the background turbulence stripped away the twist
  - $\rightarrow$ upper BC $\rightarrow$ mitigates the magnetic twist that was transported from the subsurface domain.

KYUNG HEE UNIVERSITY

Results: magnetic helicity

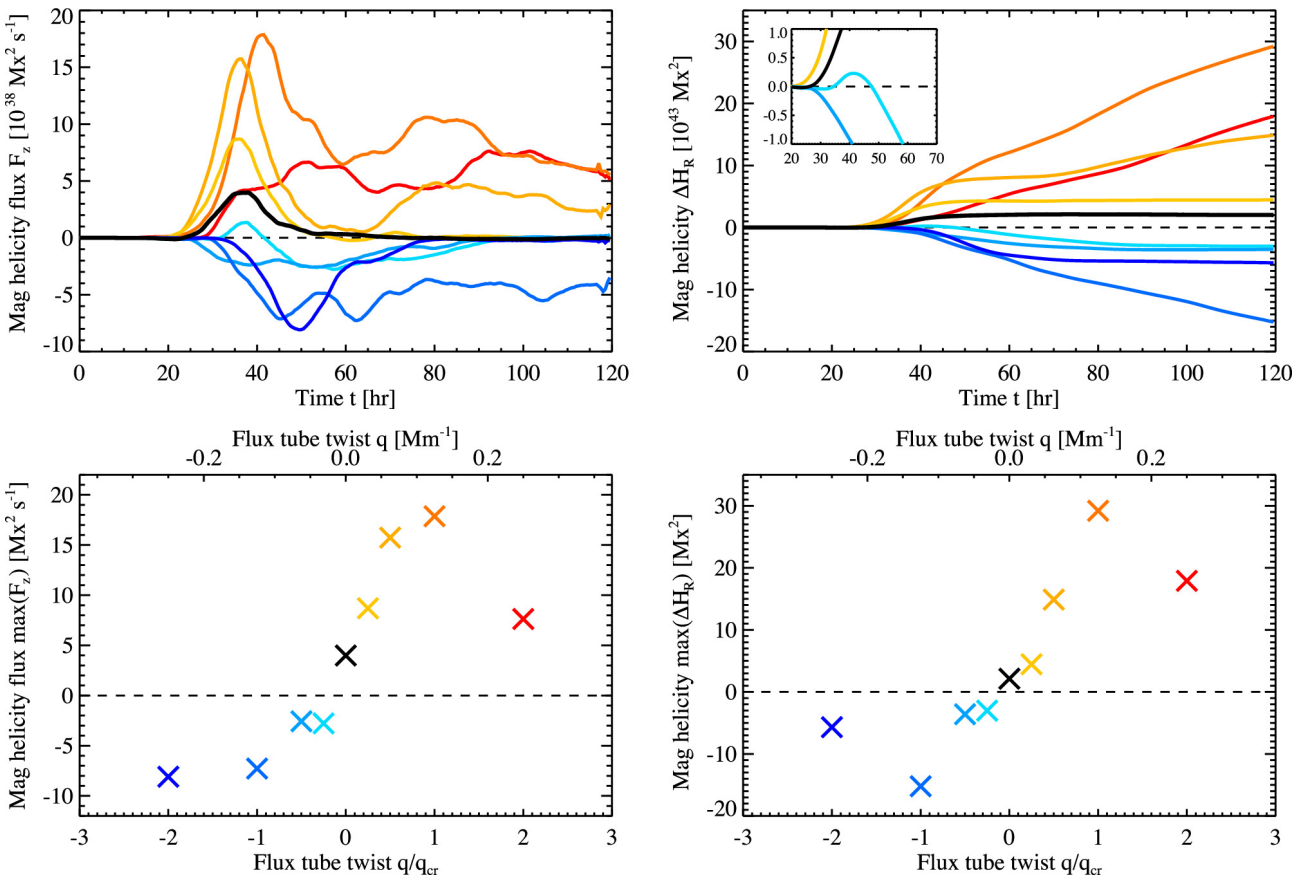

Figure 8: Temporal evolutions of the helicity flux rate, F_z, and the total injected magnetic helicity, ΔH_R. The helicity ΔH_R for the cases $q/q_{cr} = [1/4, 0, -1/4, -1/2]$ are also shown in the inset. (Bottom panels)

KYUNG HEE UNIVERSITY

Results: magnetic helicity

- Peak values decrease as twist strength decreases.
- Even the no-twist case injects finite (positive) helicity.
- In the $q/q_{cr} = -1/4$ case, helicity briefly swings positive before steadily going negative.
  - $\rightarrow$ competition between the positive helicity added by the background convection and the counteracting negative magnetic helicity of the original flux tube.

KYUNG HEE UNIVERSITY

Results: Normalized magnetic helicity

- In comparing with observations, a normalized helicity measure ($\Delta H_R/\Phi^2$) is used.
- Observations show that the typical value of the normalized helicity, $\Delta H_R/\Phi^2$, is of the order of 0.01.
  $\rightarrow$ super-flaring ARs $\rightarrow \Delta H_R/\Phi^2 \leq 0.04$
- For $|q/q_{cr}| = 1/2$, values already excced the observed level (> 0.1)
- Twist above the kink threshold ($|q/q_{cr}| > 1$) leads to unrealistically large helicity.

KYUNG HEE UNIVERSITY

Results: Magnetic energy

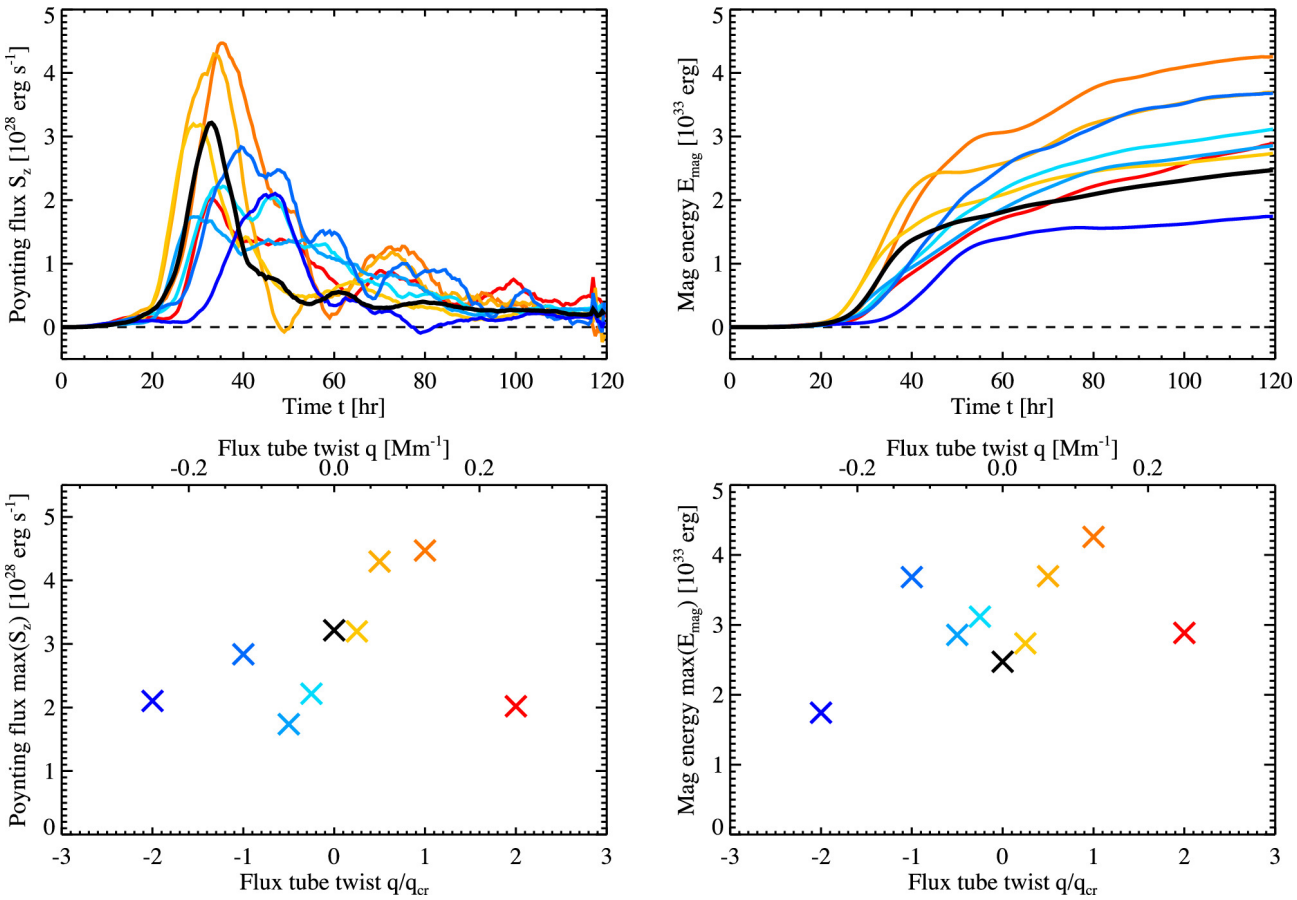

Figure 9: Temporal evolutions of the Poynting flux in the photosphere, S_z, and the injected magnetic energy, E_{mag}. Their peak values as a function of the initial flux tube twist, q/q_{cr}.

Results: Magnetic energy

- Cases with $q/q_{cr} = 1$ and $1/2$ achieve the highest peaks.
- The $q/q_{cr} = -1$ case shows a large peak value of $max(E_{mag})$
  $\rightarrow$ continued injection of the S_z, although $max(S_z)$ is low.
- E_{mag} tends to increase with the increase of $|q/q_{cr}|$
  $\rightarrow$ $max(S_z)$ is larger
  $\rightarrow$ emergence continues
- For $|q/q_{cr}| = \pm 2$, E_{mag} is not remarkable because the flux emergence fails.

KYUNG HEE UNIVERSITY

Discussion & conclusion: key findings

- **Magnetic flux emergence:**
  - → Flux tubes reach the photosphere via convective upflows, regardless of twist.
  - → If twist is too weak, flux disperses rapidly in the photosphere.
- **Magnetic twist:**
  - → Photospheric measurements largely preserve the initial twist.
  - → Within realistic observational ranges.
- **Magnetic helicity:**
  - → Even untwisted tubes gain helicity from background turbulence.
  - → Twist above the kink threshold produces unrealistic helicity levels.

KYUNG HEE UNIVERSITY

Discussion & conclusion: theoretical implications

- **δ-Spot Formation Mechanism:**
  - $\rightarrow$ Kink instability may not be the primary mechanism for δ-spot formation.
  - $\rightarrow$ Other scenarios: multiple flux tube interactions, multi-buoyancy-segment tubes, etc.
- **Role of convection:**
  - $\rightarrow$ Convection is a non-negligible source of helicity.
  - $\rightarrow$ Confirms the importance of twist in preserving flux tube integrity.
- **Magnetic energy transport:**
  - $\rightarrow$ Less than 10% of initial tube energy reaches the upper atmosphere.
  - $\rightarrow$ Most of the magnetic energy remains in the convection zone.

KYUNG HEE UNIVERSITY

Discussion & conclusion: limitations and future work

- **Study Limitations:**
  - → Difficult to confirm kink instability fully.
  - → Need to account for different initial tube positions.
- **Future Directions:**
  - → Expand the parameter space.
  - → Investigate alternative -spot formation mechanisms.

KYUNG HEE
UNIVERSITY

Thank you for listening!

Questions?

KYUNG HEE UNIVERSITY